Effect of Rheology and Heat Transfer on Food 3D Printing Performance

Pietro Rando[1], Joseph L. Keddie[2] and Marco Ramaioli[1,3]

[1] Department of Chemical and Process Engineering, University of Surrey, GU2 7XH, Guildford,UK
[2] Department of Physics, University of Surrey, GU2 7XH, Guildford, UK
[3] UMR SayFood, Université Paris-Saclay, AgroParisTech, INRAE, 78850, Thiverval Grignon, France

ABSTRACT

Food 3D printing, is an additive manufacturing process in which three dimensional edible products with customized shapes and structure are built layer by layer.

The relationship between the material's rheological and heat transfer properties and the process conditions was investigated, to predict the stability of 3D printed structures. IR thermography allowed measuring in-situ the cooling kinetics of the printed material that is interpreted using a heat transfer model. Finally, a model based on the yielding has been proposed to understand the conditions leading to a stable structure or to a collapse.

The results show that the printing velocity, the environmental temperature play a crucial role to ensure an appropriate cooling and structure stability.

INTRODUCTION

In the past years, 3D printing found application in food manufacturing, giving a tool to design and create products with customized shape and texture.[1] Food products can be designed and fabricated to meet individual needs through controlling the amount of material and nutrition content.[2] Several food formulations have been used to manufacture 3D printed structures such as mash potatoes,[4] starch based products[5],[6] pectin based foods,[7] surimi,[8] food gels,[9] sodium caseinate,[10] vegetables and fruit blends[11] and even healthy snacks for children.[12]

Food 3D printers often employ an extrusion mechanism, where many phenomena occur simultaneously: the process is non-isothermal, the materials flowing in the nozzle are non-Newtonian, sintering occurs between different layers, and the extruded material solidifies after deposition. The printing parameters affect the material rheological, heat and mass transfer properties.

Extrusion based 3D printing of plastic polymers such as polylactic acid (PLA)[13] and acrylonitrile butadiene styrene (ABS)[1617],[14] has been studied in depth in the literature. The material temperature is a key parameter during the object manufacturing. In fact, the printing material must be in a molten state when it flows through the nozzle; whereas, after deposition, it cools down and solidifies to guarantee the stability of the 3D printed structure, drastically increasing its viscosity, which follows an Arrhenius law[13] or a Williams-Landel-Ferry model.[15] Usually, molten polymers or suspensions used in 3D printing show a shear-thinning behaviour.[13] The nozzle opening is placed at a 90° angle respect to the build plate and the shape of the deposited filaments is considered elliptical since the layer thickness is usually lower compared to the nozzle diameter[15].[17] In order for the layers to bond the temperature at the filaments' interface has to be higher than the glass transition temperature or crystalline melting temperature. A model to describe ABS filament welding has been used by Bellehumeur *et al.*,[16],[17] who considered a Pokluda model for Newtonian fluids to study the bridge growth between filaments. Sun *et al.*[16] measured experimentally the temperature layer deposition of ABS filaments using thermocouples and proposed a heat transfer model to predict the filament temperature. Different printing parameters were investigated, finding that the "printing strategy" and build plate temperature significantly affect the filaments cooling dynamics. Seppala *et al.*[14] used a IR camera as alternative technique to thermocouples to measure the filament surface temperature in proximity the neck between the two layers.

Chocolate has been often used in food extrusion-based 3D printing because after deposition it solidifies allowing to build 3D structure that self-support[1] themselves under the weight applied from the upper layers. Chocolate is a dense suspension of non-fat particles like sugar and cocoa solids dispersed in a continuous phase of cocoa butter.[18] Molten chocolate is a non-Newtonian fluid characterized from shear-thinning behaviour, yield stress and a small degree of tixotropy. The yield stress can be obtained from fitting extrapolation form the Casson model, as recommended from International Confectionery Agency (ICA) or the Herschel-Bulkley model.[19] Oscillatory rheology, through stress sweep, were used to predict the yield stress of chocolate mixtures, identified as the critical stress at the end of the linear viscoelastic region.[20]

A chocolate 3D printer has been fabricated from Hao *et al.* who studied the effect of different printer settings and identifies nozzle diameter, nozzle height and extrusion rate as key parameters for the 3D printing of a milk chocolate mixture.[21] Lanaro *et al.* presented the design of a chocolate 3D printer and optimize cooling rate of chocolate filaments, using an air cooler, placed at the nozzle exit to improve the ability of chocolate layers to solidify and manufacture self-supporting structures.[22] Mantihal *et al.* studied the effect of the geometry and internal structure of chocolate 3D printed product on their texture and self-support properties.[23]

In this work, we have investigated the link between material's heat and rheological properties and the process parameters, in order to predict the structure stability. IR thermography was used to measure experimentally the temperature profiles of the extruded material after deposition at different printing speeds and build plate temperatures. The understanding provided by this study can help optimising the printing conditions of product formulation to guarantee a satisfactory printing performance.

EXPERIMENTAL

A dark chocolate BC-811 (Barry Callebaut, UK), containing 37.8% fat and 54.5% cocoa solids, was used as printing material. Before printing, chocolate has been tempered, using a Mini Rev Tempering Machine (ChocoVision, UK), increasing the chocolate temperature from 20 to 45 $°C$, to melt the cocoa butter crystals and then cooled down to the printer nozzle temperature ($T_n = 32°C$).

The molten chocolate rheological behaviour has been characterized using a rotational rheometer Paar-Physica UDS2000 and a cone and plate geometry (d = 23 mm ; $\theta = 2°$; gap = 50 μm). The shear rate was varied between 1 and 60 s^{-1}, based on the theoretical estimation of the capillary flow in the nozzle diameter of the printer ($d_n = 0.8$ mm). The measurement were performed at 32 and 26 $°C$. At lower temperature the cocoa butter crystallizes. Each test was repeated three times.

Finally the yield stresses, τ_0, has been obtained by fitting the shear stress (τ) versus the shear rate ($\dot{\gamma}$) using a Herschel-Bulkley model:[19]

$$\begin{cases} \tau < \tau_0, & \dot{\gamma} = 0 \\ \tau > \tau_0, & \tau = \tau_0 + K\dot{\gamma}^n \end{cases} \tag{1}$$

A Choc Creator V2.0 Plus (Choc Edge Ltd, UK) 3D printers was used to manufacture 3D structures by extruding thin layers of molten chocolate from a moving heated nozzle onto a building plate. After tempering the molten chocolate was loaded into a steel syringe equipped with a 0.8 mm nozzle, which is wrapped in a heated jacket, to keep the temperature constant at $T_n = 32°C$.

A simple *"wall geometry"*, reported in Figure 1, consisting of 16 layers (L = 7 cm, h_{layer} = 0.6 mm and h = 1 cm) deposited on the top of each other has been designed, using FREECAD software. Afterwards, it was imported in the printer's slicer software were the printing parameters have been set and a G-code, containing information on the printing path, printing velocity and amount of extruded material was automatically generated. During printing, chocolate filaments were extruded from the nozzle when it moves from $y = 0$ to $x = L$ at a set V_p; whereas the nozzle was translated without extrusion in the opposite direction at a travel velocity V_t, from $y = L$ to $y = 0$.

Printing conditions were varied in order to investigate their effect during the layers cooling and the self-supporting stability of the printed structures. The tested parameters such as build plate temperature (T_e), printing (V_p) and travel velocity V_t are reported in table 1.

Table 1. Summary of printing parameters tested during the manufacturing of 3D structures.

Operating Conditions	Range
T_n	32 $°C$
T_e	[18-22] $°C$
V_p	[4-16] mm/s
V_t	[4-12] mm/s

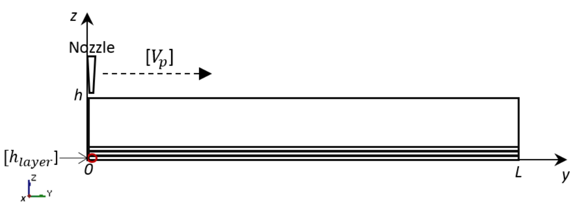

Figure 1. 2D Sketch of the 3D printed wall structure with its dimensions. The region where the temperature profile was evaluated is highlighted in red.

The temperature profiles of the deposited chocolate, during the 3D printing process on different part of the structures' surface, using a IR Camera Testo 885 (S.A. Testo N.V, Belgium), placed in front of the build plate, imaging the y-z plane. During the structure manufacturing, video were recorded at a frame rate of 33 Hz and a resolution of 320x240 pixel. The red circle, in Figure 1, represents the point where the temperature profiles were measured over time. Finally, the height of the structure has been measured at after the deposition of each layer, using ImageJ. Every test was repeat in triplicate.

RESULTS AND DISCUSSION

The stability or collapse of the printed structures will be discussed followed by the effect of different environmental temperature and printing velocities on the cooling kinetics. Finally a simple heat transfer model to predict the filament cooling after deposition will be presented.

Stability of 3D Printed Structures

The environmental temperature and printing speed have been varied systematically in order to identify which conditions can lead to a successfully manufacturing 3D chocolate structures and in which condition a collapse occurs. We found that at a room temperature of 18 $°C$, it was possible to manufacture structure at a printing speed between 4 and 12 mm/s since the cocoa butter crystallizes; whereas at a velocity of 16 mm/s the deposited material does not have enough time to cool down and the structure collapses. At a T_e equal of 20 $°C$, it was possible to build structures only at a velocity of 4 mm/s since printing time is high and the cocoa butter at the base of the structure has enough time to crystallize. Finally, at a T_e of 22 $°C$ cocoa butter does not have time crystallize leading to a collapse of the structure, even at the lowest printing velocity $V_p = 4mm/s$.

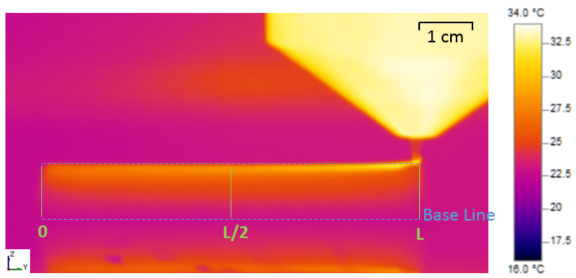

Figure 2. Temperature distribution of a 3D printed structure.

In Figure 2 is reported a IR image of a 3D printed structure, showing that the temperature is not uniform, due to boundary effects. In fact, it is possible to identify a colder region where the heat exchange with the build plate occurs and a warmer region on the top of the structure. Moreover, in the middle of the structure the temperature is slightly higher. In table 2 are reported the values of height (h_c), time (t_c) and temperature of collapse (T_c), measured experimentally at the conditions which lead to the collapse of the structure. Measurements were taken along the coordinate $y = L/2$. All the collapses occur above the base of structure, where the heat exchange is not quick enough and therefore the deposited material takes longer to cool down.

Table 2. Printing conditions leading to the structure collapse: temperature (T_c), height (h_c) and time (t_c) of collapse.

T_e [°C]	V_p [mm/s]	T_c [°C]	h_c [mm]	t_c [s]
18	16	25.0	0.225	121.0
20	8	24.7	0.269	245.0
22	4	26.5	0.284	183.7

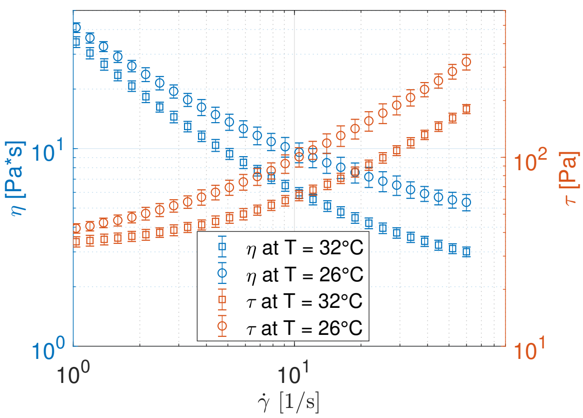

Figure 3. Chocolate viscosity and shear stress varying with the shear rate at different temperature: T = 32 °C (dots) and T = 26 °C (squares).

Chocolate viscosity (η), reported in Figure 3, drops when the shear rate ($\dot{\gamma}$) increases showing a shear-thinning behaviour; whereas the shear stress (τ) increases with the shear rate. Moreover, at a temperature of 26 °C the viscosity and the shear stress increase due to the partial crystallization of cocoa butter. Values of the yield stress and consistency index of chocolate have been estimated from the Herschel-Bulkley model (Eq. (1)). Results are summarized in table 3 and show a good agreement with the model. It is possible to observe that at a temperature of 26 °C the values of the yield stress and the consistency index are higher due to the partial crystallization of cocoa butter. It was chosen to fit a single value of n equal to 0.9.

Table 3. Rheological parameters by fitting the Herschel-Bulkley model.

$T[°C]$	$\tau_0[Pa]$	$K[Pa \cdot s^n]$	n	R^2
32	31.75	3.38	0.9	0.9894
26	38.28	7.17	0.9	0.9987

The step-wise increase in the stress acting on the base of the structure (σ_{theo}), due to the weight of the deposited material can be expressed as Eq. (2) where ρ and g are respectively the chocolate density and the gravity.

$$\Delta\sigma_{theo} = \rho g h_{layer} \qquad (2)$$

In Figure 4 is reported a comparison between the maximum theoretical (σ_{theo}) stress predicted from the theoretical structure height and σ_{exp} computed using the height measured experimentally when the printing speed is 4 mm/s and $T_e = 22°C$. The stress was evaluated at the fourth layer of the structure. The values of σ_{exp} match the theoretical values during the deposition of additional four layers. At the next step, however, $\sigma_{exp} < \sigma_{theo}$, indicating that the material is flowing towards the bottom, due to the gravity. Finally, when the height exceeds the yield stress at T= 26 °C (dotted line, $\tau_{0,T=26°C}$) the stress due to the weight of the structure leads to the collapse.

Influence of Environmental Temperature

The room temperature, T_e, has been varied between 18 °C and 22 °C. The temperature profiles, measured at the origin of the structure $(y,z) = (0,0)$, are shown in Figure 5. The printing time has been normalized, dividing by the characteristic process time: defined as the time needed to return to the same y-coordinate, $(\tau_p = \frac{L}{V_p} + \frac{L}{V_t})$.

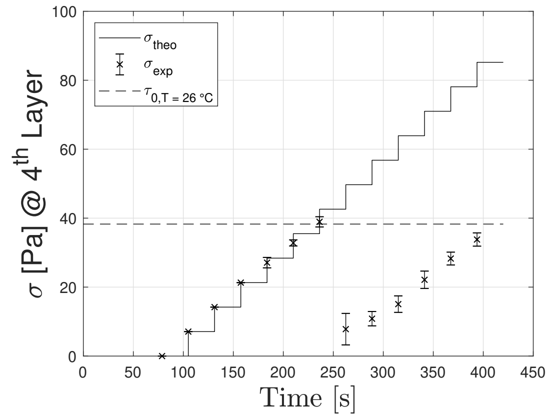

Figure 4. Comparison between theoretical (continuous line) and experimental stresses (cross dots) acting on the 4^{th} layer of the structure and the yield stress (dotted line). $T_e = 22°C$ and V_p = 4 mm/s.

The temperature profiles show a periodical trend, where the temperature initially fluctuates, due to the deposition of new hot material on the same y-coordinate, and after the deposition of the forth layer reaches equilibrium. It was found that when the T_e increases, the temperature reached by the material at long times is higher.

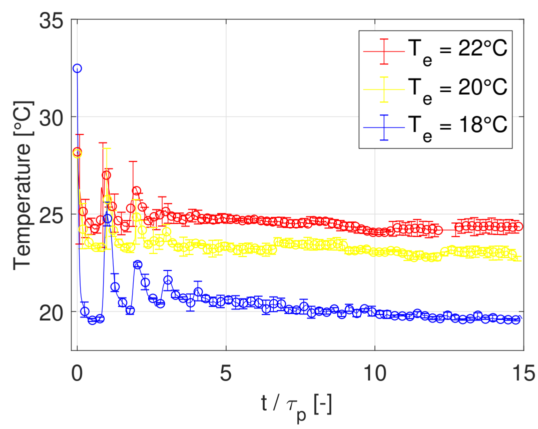

Figure 5. Temperature profiles measured at the structure origin, at T_n = 32 °C and V_p = 4 mm/s at different room temperature respectively T_e = 22 °C (red), T_e = 20 °C (yellow), T_e = 18 °C (blue).

Influence of Printing Speed and Heat Transfer Model

The printing speed has been varied from 4 to 12 mm/s, keeping constant the nozzle and a room temperature. Furthermore, a simple model, proposed from Bellehumeur *et al.*[17] (Eq. (3)), has been adapted to investigate the cooling behaviour of deposited filaments.

$$T = (T_n - T_e) \cdot exp\left(-\frac{t}{\tau_c}\right) + T_e \tag{3}$$

where τ_c was defined as the characteristic cooling time and depends on geometry, process conditions and the heat transfer coefficient. The values of τ_c have been estimate fitting Eq. (3), for the first cycle of cooling. Results are reported in table 4. It has been found that increasing the printing velocity the characteristic cooling time increases, since more material has to cool down through the same bottom surface.

A comparison between the model and the experiments, during the first cycle is reported in Figure 6. Temperature and time have been previously normalized. It is possible to see that the temperature reaches the equilibrium in approx. 40% of τ_p, and increasing the printing speed slows down the cooling kinetics. Experimental data have good agreement with the heat transfer model.

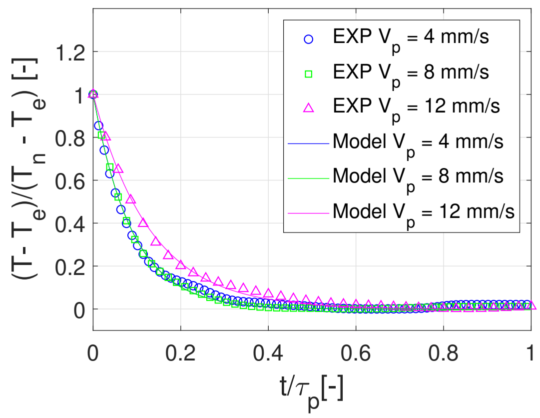

Figure 6. Comparison between experiments (dots) and heat transfer model (line) of cooling profiles for a $T_e = 18°C$ at different printing speed: V_p = 4 mm/s (blue), V_p = 8 mm/s (green), V_p = 12 mm/s (magenta).

Table 4. Characteristic cooling time, τ_c, during the deposition of the first filament at $T_e = 18°C$.

V_p [mm/s]	$\tau_{c,1^{st} layer}$ [s]
4	0.055
8	0.071
12	0.116

SUMMARY AND CONCLUSIONS

In this work, the effect of different process conditions on the stability of 3D printed edible structures was investigated. An IR camera has been used to quantify locally the temperature on the structures' surface, during the printing process, and the experimental data have been interpreted with a simple heat transfer model to predict the cooling dynamics of 3D printed chocolate filaments.

Experimental results show that the cooling kinetics of the deposited material and the overall structure stability were mainly affected by the environmental air temperature, build plate temperature and printing velocity. To manufacture stable structures, during the cooling kinetics of the extruded material, in every part of the structure the yield stress should be higher than the applied vertical stress. A simple model to estimate the maximum theoretical stress supported from the local yield stress has been proposed, in agreement with the experimental data.

The results of this paper can be useful to optimize the printing condition based on the heat and rheological properties of printing material formulation.

REFERENCES

1. Fernanda C. Godoi, Sangeeta Prakash, Bhesh R. Bhandari (2016) *3D printing technologies applied for food design: Status and prospects.* Journal of Food Engineering (Vol. 179, pp. 44-54).

2. Jie Sun, W. Zhou, D. Huang, Jerry Y.H. Fuh, Geok Soon Hong (2015) *An Overview of 3D Printing Technologies for Food Fabrication.* Food Bioprocess Technol. 8 (8), pp 1605-1615.

3. Zhenbin Liu , Min Zhang, Bhesh Bhandari, Yuchuan Wang. (2017), *3D printing: Printing precision and application in food sector* Trends in Food Science and Technology 69 (2017) 83 - 94.

4. Z. Liu, M. Zhang, B. Bhadari, C. Yang (2017) *Impact of Rheological Properties of Mash Potatos on 3D Printing.* Journal of Food Engineering (pp 1-7).

5. Zhenbin Liu, Bhesh Bhandari, Sangeeta Prakash, Sylvester Mantihal, Min Zhang (2019) *Linking rheology and printability of a multicomponent gel system of carrageenan-xanthan-starch in extrusion based additive manufacturing.* Food Hydrocolloids 87 (2019) 413 – 424.

6. Huan Chen, Fengwei Xie, Ling Chen, Bo (2019), *Effect of rheological properties of potato, rice and corn starches on their hot- extrusion 3D printing behaviors* Journal of Food Engineering 244 (2019) 150–158.

7. Valerie Vancauwenberghe, Louise Katalagarianakis, Zi Wang, Mathieu Meerts, Maarten Hertog, Pieter Verboven, Paula Moldenaers, Marc E. Hendrickx, Jeroen Lammertyn, Bart Nicolai (2017) *Pectin based food-ink formulations for 3D printing of customizable porous food simulants*, Innovative Food Science & Emerging Technologies, Volume 42, 2017, Pages 138 - 150.

8. Lin Wang, Min Zhang, Bhesh Bhandari, Chaohui Yang *Investigation on fish surimi gel as promising food material for 3D printing*, Journal of Food Engineering, Volume 220, 2018, Pages 101-108

9. Yang, Fanli Zhang, Min Bhandari, Bhesh Liu, Yaping (2017) *Investigation on lemon juice gel as food material for 3D printing and optimization of printing parameters.* LWT - Food Science and Technology (Vol.87, pages 67-76).

10. M.A.I. Schutyser, S. Houlder, M. de Wit , C.A.P. Buijsse , A.C. Alting (2018) *Fused deposition modelling of sodium caseinate dispersions.* Journal of Food Engineering 220 pp 49-55.

11. C. Severini, A. Derossi, I. Ricci, R. Capor-

izzi, A. Fiore (2017) *Printing a blend of fruit and vegetables. New advances on critical variables and shelf life of 3D edible objects.* Journal of Food Engineering.

12. A. Derossi, R. Caporizzi, D. Azzollini, C. Severini (2016) *Application of 3D printing for customized food. A case on the development of a fruit-based snack for children.* Journal of Food Engineering (pp. 1-11).

13. Brian N. Turner, Robert Strong, Scott A. Gold, (2014) *A review of melt extrusion additive manufacturing processes: I. Process design and modeling*, Rapid Prototyping Journal (2014), Vol. 20 Issue: 3, pp.192-204.

14. Jonathan E. Seppala, Kalman D. Migler (2016) *Infrared thermography of welding zones produced by polymer extrusion additive manufacturing* Additive Manufacturing 12 (2016) 71–76.

15. Claire McIlroy and Peter D. Olmsted (2017) *Deformation of an Amorphous Polymer during the Fused-Filament-Fabrication Method for Additive Manufacturing* Journal of Rheology 61, 379.

16. Q. Sun, G.M. Rizvi, C.T. Bellehumeur and P. Gu (2008) *Effect of processing conditions on the bonding quality of FDM polymer filaments* Rapid Prototyping Journal 14/2 (2008) 72-80.

17. Bellehumeur , Longmei, Qian , Peihua (2004) *Modeling of Bond Formation Between Polymer Filaments in the Fused Deposition Modeling Process*, Journal of Manufacturing Processes Vol. 6/No.2 2004.

18. Beckett, S. T., (2009) *Industrial Chocolate Manufacture and Use.* 4th ed. s.l.:Wiley-Blackwell.

19. Ahmet Sokmen, Gurbuz Gunes(2006) *Influence of some bulk sweeteners on rheological properties of chocolate*. LWT - Food Science and Technology 39 pp. 1053–1058.

20. Veerle De Graef, Frédéric Depypere, Maaike Minnaert, Koen Dewettinck(2011) *Chocolate yield stress as measured by oscillatory rheology*. Food Research International 44 pp. 2660 - 2665.

21. L. Hao , S. Mellor , O. Seaman , J. Henderson , N. Sewell , M. Sloan (2010) *Material characterisation and process development for chocolate additive layer manufacturing.* Virtual and Physical Prototyping (Vol.5, issued 2, pages 57-64).

22. Matthew Lanaro, David P. Forrestal, Stefan Scheurer, Damien J. Slinger, Sam Liao, Sean K. Powell, Maria A. Woodruff (2017) *3D printing complex chocolate objects: Platform design, optimization and evaluation.* Journal of Food Engineering (Vol. 215, pages 13-22).

23. Sylvester Mantihal, Sangeeta Prakash, Fernanda Condi Godoi, Bhesh Bhandari (2017) *Optimization of chocolate 3D printing by correlating thermal and flow properties with 3D structure modeling.* Innovative Food Science and Emerging Technologies 44 (2017) 21 – 29.